Available online at www.sciencedirect.com
SCIENCE DIRECT®
Journal of Solid State Chemistry 177 (2004) 4067–4072
JOURNAL OF SOLID STATE CHEMISTRY
www.elsevier.com/locate/jssc

Structural and electrical changes in $NdSrNiO_{4-\delta}$ by substitute nickel with copper

Hanèn Chaker[a], T. Roisnel[b], M. Potel[b], R. Ben Hassen[a,*]

[a] *Unité de Recherche de Chimie des Matériaux, Faculté des Sciences de Sfax B.P. 802, Universite de Sfax, 3038 Sfax, Tunisia*
[b] *Laboratoire de Chimie du Solide et Inorganique Moléculaire, UMR 6511 CNRS-Université de Rennes 1, Institut de Chimie de Rennes, Avenue du Général Leclerc 35042 Rennes Cedex, France*

Received 8 April 2004; received in revised form 11 June 2004; accepted 13 June 2004
Available online 7 October 2004

Abstract

A novel series of the formula $NdSrNi_{1-x}Cu_xO_{4-\delta}$ were synthesized for various values of x ranging from 0 to 1 in 1 atm of O_2 gas flow using conventional solid-state methods and were characterized by powder X-ray diffraction and electrical resistivity measurements. The compounds have been shown to adopt the K_2NiF_4-type structure. The oxygen stoichiometry of the compounds was determined from thermo-gravimetric analysis (TGA). An analysis of the micro-structure of the neodymium strontium nickel copper oxide is described. All the samples were semi-conducting from room temperature down to 77 K. The effect of Cu^{2+} incorporation on the structural and electrical properties of $NdSrNi_{1-x}Cu_xO_{4-\delta}$, $0 \leqslant x \leqslant 1$, are discussed in terms of Jahn–Teller distortion of the $(Ni/Cu)O_6$ octahedra and mixed valence character of copper.

Keywords: X-ray powder diffraction; K_2NiF_4-type structure; Rietveld refinement; Oxygen content; Micro-structure study and resistivity measurements

1. Introduction

Many mixed oxides of the type A_2BO_4 (A = rare earth, alkaline-earth; B = transition metal) crystallize with the tetragonal K_2NiF_4-type structure (space group $I4/mmm$). As shown in Fig. 1, the structure of A_2BO_4 can be described as an ordered intergrowth of alternating perovskite (ABO_3) and rock salt (AO) layers stacked along the tetragonal c-axis. The BO_6 octahedra share corners in the ab plane forming a two-dimensional array of B–O–B bonds which is responsible for a variety of interesting physical phenomena, as for example, the anisotropic electrical transport and magnetic exchange interactions [1,2].

Rare earth nickel oxides with the general formula $Ln_2NiO_{4+\delta}$ (Ln = La, Pr or Nd) are known to crystallize with K_2NiF_4-type structure. It is reported that $Nd_2NiO_{4+\delta}$ can have either monoclinic [3] or orthorhombic symmetry [4]. The source of the structural difference is unclear, it may be due to the oxygen content or structural defects. It has also been reported that $NdSrNiO_4$ has tetragonal symmetry [5,6]. It was thought that the substitution of Nd by Sr in $Nd_2NiO_{4+\delta}$ might induce a structural phases transition from orthorhombic to tetragonal symmetry leading to a mixed valence for the transition metal ion, which would in turn induce interesting electrical and magnetic properties in this system. The high temperature structural phase transition observed for $Nd_2NiO_{4+\delta}$ at 847 K was suppressed rapidly with the incorporation of Sr^{2+} in the structure. All the members of the solid-solution series of $Nd_{2-x}Sr_xNiO_{4+\delta}$, $0 \leqslant x \leqslant 1$ are semi-conducting down to 10 K, except for $NdSrNiO_4$, which undergoes a metal to semi-conductor transition at 190 K [7].

*Corresponding author. Fax: +216-74-274-437.
E-mail address: rached.benhassen@fss.rnu.tn (R.B. Hassen).

0022-4596/$ - see front matter © 2004 Elsevier Inc. All rights reserved.
doi:10.1016/j.jssc.2004.06.028

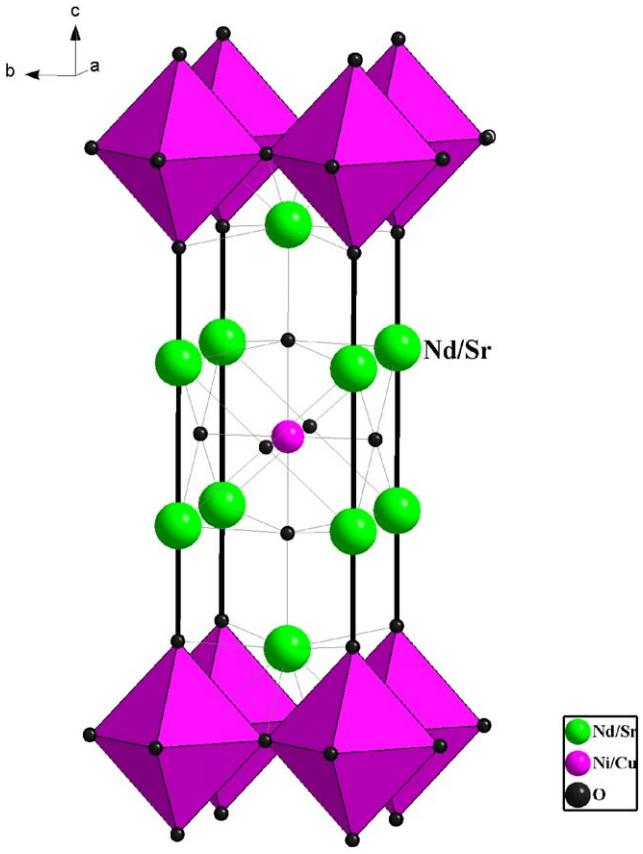

Fig. 1. Tetragonal K_2NiF_4-type structure of $NdSrNi_{1-x}Cu_xO_{4-\delta}$, $0 \leqslant x \leqslant 1$.

New interest in compounds of the formula Ln_2CuO_4 (Ln = lanthanide) has been generated by the discovery of high-temperature superconductivity in doped La_2CuO_4 [8]. The superconducting properties of this compounds generally have been considered to be dependent on the oxygen stoichiometry of the material and/or a variability of valencies of the Cu atoms [9].

Because of the isotypies in the structures of La_2NiO_4 and La_2CuO_4 (the parent compound of the discovered high temperature superconducting cuprate family), as well as reports of possible superconductivity in $La_{2-x}Sr_xNiO_{4+\delta}$ [10], recently several studies have been carried out on the structural and physical properties of $Nd_{2-x}Sr_xNiO_{4+\delta}$ in order to better understand the nature of these rare earth nickelates, in addition to the structurally related superconducting cuprates [7,11–15]. A systematic substitution of Ni by Cu has not yet been reported. The aim of this work is to investigate the effect of cupper incorporation on the structural, microstructural and physical properties of $NdSrNi_{1-x}Cu_xO_{4-\delta}$, $0 \leqslant x \leqslant 1$ system.

In this work, we have synthesized new compounds in the $NdSrNi_{1-x}Cu_xO_{4-\delta}$, $0 \leqslant x \leqslant 1$, system. We report here some preliminary results of powder X-ray diffraction, thermo-gravimetric analysis (TGA) and resistivity measurements. In addition, a short description of the mean crystallite sizes and anisotropy is given.

2. Experimental

Solid solutions of $NdSrNi_{1-x}Cu_xO_{4-\delta}$, $0 \leqslant x \leqslant 1$, were prepared in polycrystalline form by conventional solid-state methods. Prior to use, Nd_2O_3 (Aldrich 99.99%) was calcined at 1100 °C for 9 h in air to remove any hydrogeno-carbonate impurities. NiO and CuO (Aldrich 99.99%) were used as obtained. Stoichiometric amounts of Nd_2O_3, $SrCO_3$, NiO and CuO were thoroughly ground together and calcined at 950 °C for 24–36 h in 1 atm of O_2 gas flow in order to reach oxygen stoichiometry. The powders were finally uniaxially cold pressed into pellets and sintered at 1150 °C for an additional period of 4 days usually with two intermittent grindings. The samples were cooled to 600 °C in the furnace before being quenched to room temperature. Powder X-ray diffraction data for the six samples ($x = 0$, 0.2, 0.4, 0.6, 0.8, and 1) were collected at room temperature using a Siemens D500 diffractometer, with a monochromatic Cu$K\alpha_1$ radiation ($\lambda = 1.54056$ Å) obtained with an incident-beam curved germanium monochromator. Data were collected with a 0.02° step 2θ width and 50 s counting time per point over a 2θ range from 12° to 62° and for 100 s over a 2θ range from 62.02° to 114°. Data are then normalized to a constant acquisition time and count e.s.d.'s calculated consequently. The pattern matching and Rietveld refinements were performed with FULLPROF [16].

Micro-structural features have been evaluated from a whole diffraction pattern profile analysis, using recent developments implemented in the Fullprof program [17]. Describing instrumental and intrinsic profiles by normalized Voigt function (convolution of Gaussian and Lorentzian functions), size and strain effects are separated from a whole profile pattern analysis based on different angular dependence of the Gaussian and Lorentzian full-width at half-maximum (H_G and H_L, respectively) of the sample profile, following these equations [18]:

$$H_G^2 = (U_{\text{strain-iso}} + (1-\xi)D^2_{\text{strain-aniso}})tg^2\theta + \frac{G_{\text{size-iso}}}{\cos^2\theta},$$

$$H_L = (X_{\text{strain-iso}} + \xi D_{\text{strain-aniso}})tg\theta + \frac{Y_{\text{size-iso}} + F_{\text{size-aniso}}}{\cos\theta},$$

where U, X, ξ, G and Y are refinable parameters, and D and F are analytical functions, depending on a set of additional refinable parameters, to model hkl-dependent line broadening due to strain and size effects, respectively. NIST reference LaB_6 powder was used as standard to determine the instrumental resolution

function (IRF) of our diffractometer, obtained using single line profile fitting facility implemented in WinPLOTR [19].

The total oxygen content of the samples was determined by hydrogen reduction in a TGDTA 92-SETARAM thermo-gravimetric analyser (TGA). The sample was heated in an alumina pan, in flowing 5% H_2 in N_2 gas (flow rate = 1.5 L/h) from room temperature to 1100 °C at a rate of 10 °C/min.

Electrical direct current resistivity measurements were carried out on sintered pellets in standard four-probe configuration using Van der Pauw method [20]. Measurements were performed in the temperature range 77–300 K during cooling the sample in liquid nitrogen.

3. Results and discussion

3.1. Structural study and oxygen stoichiometry analysis

The preparation of the solid solution $NdSrNi_{1-x}Cu_xO_{4-\delta}$ was attempted in the range $0 \leqslant x \leqslant 1$. Particular compositions have been synthesized: $x = 0.0$, 0.2, 0.4, 0.6, 0.8 and 1.0 leading to X-ray single phase specimens.

In order to study the variation in the oxygen deficiency as function of copper content we have carried out TGA studies in hydrogen/nitrogen atmospheres. A common feature in the reduction curves for all compositions was the observation of a step-like behavior. This kind of broad plateaus in the weight-loss curves are generally associated to the stabilization of several phases with varied oxygen stoichiometry during the reduction process [21]. Oxygen contents are calculated for all compositions from the weight loss values, assuming Nd_2O_3, SrO, and metallic Ni/Cu as final products. A representative relative weight loss curve for $NdSrNi_{0.8}Cu_{0.2}O_{4-\delta}$ is illustrated in Fig. 2. As can be seen, the reduction phenomena consists of three steps. Same behavior is observed for all mixed neodymium strontium nickel copper oxides. To assign the weight loss accompanying each cation reduction, limit compositions of the solid solution $NdSrNiO_{4-\delta}$ and $NdSrCuO_{4-\delta}$ have been also studied. This relative weight loss is additionally represented in Fig. 2. In the case of $NdSrNiO_{4-\delta}$, the reduction process is represented in two steps and interpreted as reduction of Ni^{3+} to Ni^{2+} in a first step and then Ni^{2+} to Ni^0 in a second one. It is in contrast to the case of $NdSrCuO_{4-\delta}$ in which the reduction phenomena is characterized by one step in the weight loss curve. Moreover, the measurement of the thermal signal indicates for $NdSrNiO_{4-\delta}$ the presence of exothermic phenomena at the first step and endothermic phenomena at the second one. On the contrary, the reduction of $NdSrCuO_{4-\delta}$ was characterized by only one endothermic phenomena. Considering the bi-substituted compound $NdSrNi_{0.8}Cu_{0.2}O_{4-\delta}$, the first step of reduction is accompanied by an exothermic phenomena ($\Delta H < 0$), which can be attributed to the $Ni^{3+} \rightarrow Ni^{2+}$ reduction. The two others steps are associated with two endothermic phenomena ($\Delta H > 0$) without possibility to attribute the corresponding reduction phenomena to $Ni^{2+} \rightarrow Ni^0$ or $Cu^{2+} \rightarrow Cu^0$ reductions.

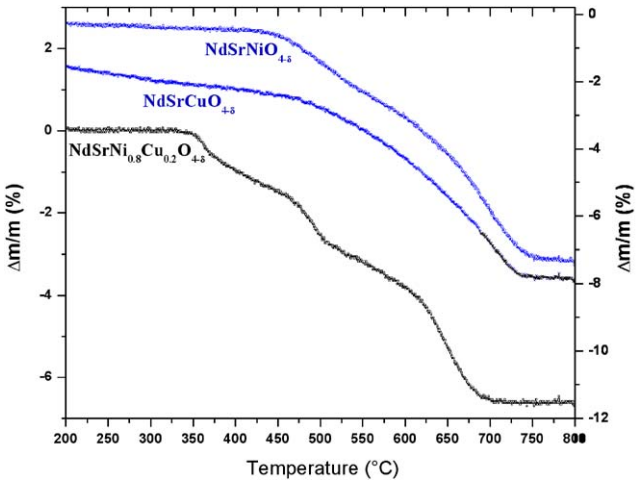

Fig. 2. Relative Weight-loss curves for $NdSrNi_{0.8}Cu_{0.2}O_{4-\delta}$, $NdSrNiO_{4-\delta}$ and $NdSrCuO_{4-\delta}$.

In addition, we note that the temperature of the reduction thresholds is systematically lowered for the bi-substituted compound compared with those of $NdSrNiO_{4-\delta}$ and $NdSrCuO_{4-\delta}$. This behavior can be related to an effect of mixed cation.

The relative weight loss, oxygen content and the copper valence calculated assuming nickel in trivalent state are given in Table 1 for all compositions. As shown in Fig. 3, the oxygen deficiency (δ) is increasing quiet linearly with increasing copper content.

Profile analysis of X-ray diffraction patterns for all compositions has been performed on the basis of a tetragonal system (space group $I4/mmm$).

The lattice parameters deduced from this whole pattern profile refinement (“pattern matching” mode in FULLPROF) of the X-ray data are presented in Table 2. The unit cell parameters for the end members ($x = 0$ and 1) agree well with those reported in the literature [14,22]. A final fit for $NdSrNi_{0.8}Cu_{0.2}O_{4-\delta}$ is displayed in Fig. 4.

The evolution of the cell parameters with the copper content x, shows the presence of a change in behavior both for a and c. The major one occurs with the c parameter, which increases from 12.2971(2) to 12.8641(2) Å versus increasing copper content. These trends in the c cell parameter can be attributed to the Jahn–Teller distortions of the Cu^{2+} ion. According to S.C. Chen et al. [23], Ni^{3+} adopts the $t_{2g}^6 d_{x^2-y^2}^1 d_{z^2}^0$ configuration in the $NdSrNiO_4$ compound. Partial substitution of Ni^{3+} by Cu^{2+}, which presents usually

Table 1
Relative weight loss, oxygen content and copper valence for all compositions

Copper content (x)	Relative weight loss (%)	Oxygen content	Cu valence
0.0	6.75(1)	3.995(8)	—
0.2	6.55(1)	3.951(7)	2.51(7)
0.4	6.25(1)	3.885(9)	2.43(4)
0.6	5.98(1)	3.826(6)	2.42(2)
0.8	5.70(1)	3.764(7)	2.41(1)
1.0	5.43(1)	3.703(8)	2.40(2)

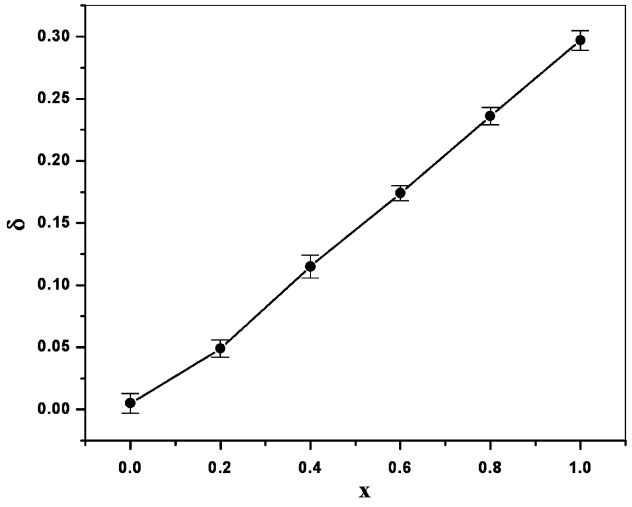

Fig. 3. Variation of oxygen deficiency (δ) as a function of x in $NdSrNi_{1-x}Cu_xO_{4-\delta}$. Continuous line is a guide for the eye.

Table 2
Unit cell parameters for mixed oxides in $NdSrNi_{1-x}Cu_xO_{4-\delta}$, $0 \leqslant x \leqslant 1$

Copper content (x)	a parameter (Å)	c parameter (Å)	Tolerance factor	Structure
0.0	3.7963(1)	12.2971(2)	0.951	T
0.2	3.7754(3)	12.4720(4)	0.935	T
0.4	3.7745(1)	12.5893(3)	0.919	T
0.6	3.7639(3)	12.6933(1)	0.904	T
0.8	3.7584(2)	12.7541(1)	0.889	T
1.0	3.7441(2)	12.8641(2)	0.875	T/O

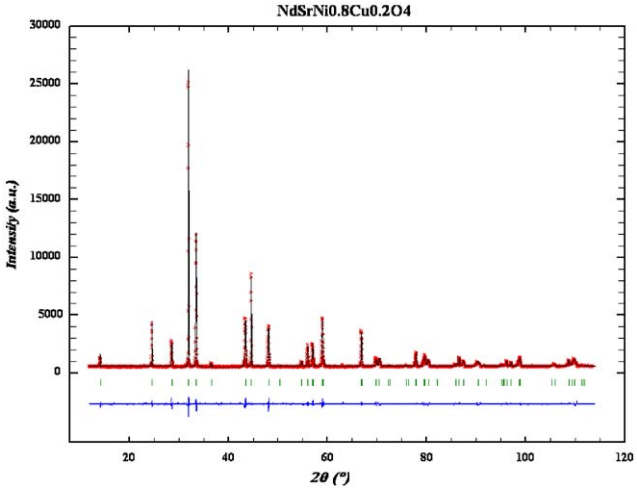

Fig. 4. Observed (crosses), calculated (continuous line) and difference X-ray diffraction patterns for $NdSrNi_{0.8}Cu_{0.2}O_{4-\delta}$. Vertical tics are related to the Bragg angles positions in $I4/mmm$ space group ($R_p = 3.9\%$, $R_{wp} = 4.9\%$ and $\chi^2 = 1.9$).

the $t_{2g}^6 d_{z^2}^2 d_{x^2-y^2}^1$ configuration in tetragonal symmetry, causes an increase only of the c parameter due to the increase on electron quantity in the $\vec{c}$ direction. The slight decrease in the a parameter is well explained by the mixed valence of copper. Indeed the Cu^{3+} adopts the $t_{2g}^6 d_{z^2}^2 d_{x^2-y^2}^0$ with deficiency of one electron in the $\vec{a}$ and $\vec{b}$ directions comparing with Cu^{2+} cation. This result is in good agreement with the assumption of Ni^{3+} oxidation state and the Cu^{2+}/Cu^{3+} mixed valence when analyzing the content of oxygen.

The stability of the $NdSrNi_{1-x}Cu_xO_{4-\delta}$, $0 \leqslant x \leqslant 1$, compounds having K_2NiF_4-type structure can be discussed in term of the value of the tolerance factor defined by Goldschmidt [24,25] as

$$t = \frac{(r_{Nd^{3+}} + r_{Sr^{2+}})/(2) + r_{O^{2-}}}{\sqrt{2}[(1-x)r_{Ni^{3+}} + xr_{Cu^{2+}} + r_{O^{2-}}]}.$$

The K_2NiF_4-type structure is stable over the range $0.866 \leqslant t < 1$. The T (tetragonal) structure exists for $0.88 \leqslant t \leqslant 0.99$ and the T/O (tetragonal/orthorhombic) structure is present for $0.866 \leqslant t < 0.88$. Based on Shannon's ionic radii [26], ($r_{Nd^{3+}} = 1.163$ Å, $r_{Sr^{2+}} = 1.31$ Å for CN = 9 and $r_{Ni^{3+}} = 0.56$ Å, in low spin case, $r_{Cu^{2+}} = 0.73$ Å for CN = 6), the calculated tolerance factors of $NdSrNi_{1-x}Cu_xO_{4-\delta}$ are $t = 0.951$, 0.935, 0.919, 0.904 and 0.889 for $x = 0.0$, 0.2, 0.4, 0.6 and 0.8, respectively. All these values are included in the tetragonal symmetry stability range. At this opposite, for the $NdSrCuO_{4-\delta}$ compound ($t = 0.875$), one can deduce structural distortion from the ideal tetragonal symmetry.

Rietveld refinements for $x = 0.2$ have been realized and confirm the K_2NiF_4-type structure. Structural refined parameters are summarized in Table 3. Oxygen stoichiometry has been fixed to the value previously determined from TGA, with oxygen deficiencies randomly distributed in both anionic sites.

3.2. Micro-structure

Detailed examination of the diffraction profile for all composition evidenced some anisotropic line broadening, i.e., hkl dependent broadening. Whole pattern refinement method implemented in Fullprof has been applied to take into account these line expansion. First refinements have been realized, modeling these

Table 3
Refined atomic parameters for $NdSrNi_{0.8}Cu_{0.2}O_{3.95}$

$NdSrNi_{0.8}Cu_{0.2}O_{3.95}$ $I4/mmm$; $a=3.7754(3)$Å, $c=12.4721(2)$Å						
Atoms	Wyckoff positions	x	y	z	B_{iso} (Å^2)	Occupation
Nd/Sr	4*e*	0	0	0.3608(1)	0.46(3)	0.5/0.5
Ni/Cu	2*a*	0	0	0	0.48(6)	0.8/0.2
O1	4*c*	0	1/2	0	0.8[a]	0.988
O2	4*e*	0	0	0.1695(6)	0.8[a]	0.988
R factors %						
R_B	7.7					
R_p	4.6					
R_{wp}	6					
R_{exp}	3.6					
χ^2	2.7					

[a]Fixed parameter.

Table 4
Mean crystallite size and size anisotropy for $x = 0.0$, 0.2, 0.4, 0.6, 0.8 and 1.0, as determined from whole profile analysis

	Mean apparent size (nm)
$x = 0.0$	29 (18)[a]
$x = 0.2$	68 (23)[a]
$x = 0.4$	102 (31)[a]
$x = 0.6$	127 (54)[a]
$x = 0.8$	155 (68)[a]
$x = 1.0$	229 (74)[a]

[a]Size anisotropy.

anisotropic line broadening by size effects, described by linear combination of spherical harmonics. Table 4 give the mean apparent size calculated by this approach, and the corresponding size anisotropy. A general trend can be extracted from these values, i.e., a particles size increase with increasing copper content. The same tendency was observed with scanning electron microscopy (SEM). Fig. 5 shows SEM micrographs of the six samples with the same scale. The study of the micro-structural features of $NdSrNi_{1-x}Cu_xO_{4-\delta}$, $0 \leqslant x \leqslant 1$, oxides obtained by solid-state reaction, has demonstrated the usefulness and consistency of the two methods for micro-structural characterization.

3.3. Electrical properties

Electrical resistivity measurements of $NdSrNi_{1-x}Cu_xO_{4-\delta}$, $0 \leqslant x \leqslant 1$, show that all the members of the solid solution are semi-conducting in the studied 77–300 K temperature range. The resistivity ρ has been fitted using the Arrhenius equation $(1/\rho) = (1/\rho_0)\exp(-E_g/2k_BT)$, which can describe a simple semi-conducting behavior. The variation of $\mathrm{Log}\,\rho$ versus $1/T$ for all compositions, is plotted in

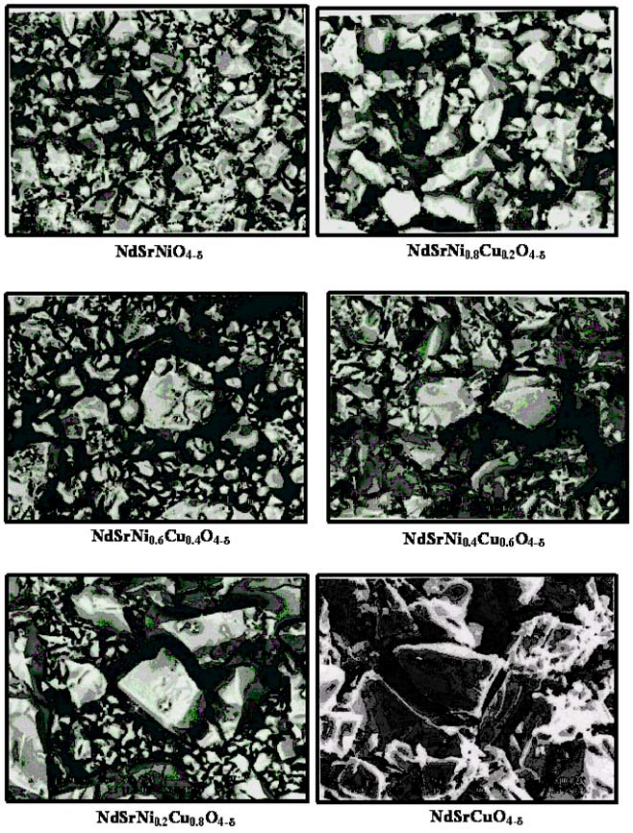

Fig. 5. SEM for $NdSrNi_{1-x}Cu_xO_{4-\delta}$ ($x = 0.0$, 0.2, 0.4, 0.6, 0.8 and 1.0).

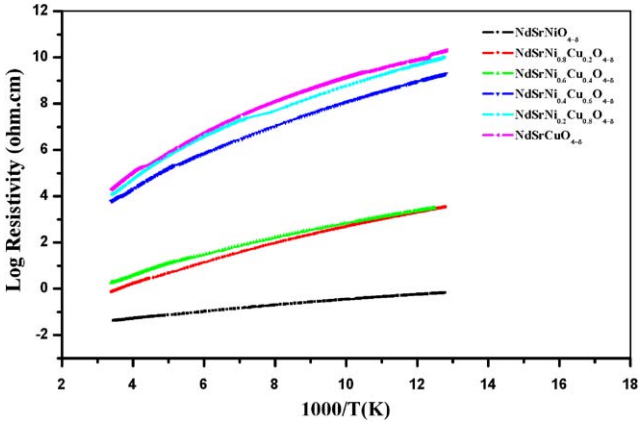

Fig. 6. Temperature dependence of $\mathrm{Log}\,\rho$ for $x = 0.0$, 0.2, 0.4, 0.6, 0.8 and 1.0 in $NdSrNi_{1-x}Cu_xO_{4-\delta}$.

Fig. 6 and shows that the electrical resistivity increases with increasing copper content.

The room temperature resistivity (ρ_{RT}) values as a function of copper content x are presented in Fig. 7. As can be seen, the room temperature resistivity is constant up to $x \approx 0.4$, then increases rapidly with x, i.e., when the formal valence of copper decreases. According to Arbuckle et al. [7], the half-filled $\sigma^*_{x^2-y^2}$ band is responsible for the metallic behavior of the $NdSrNiO_4$

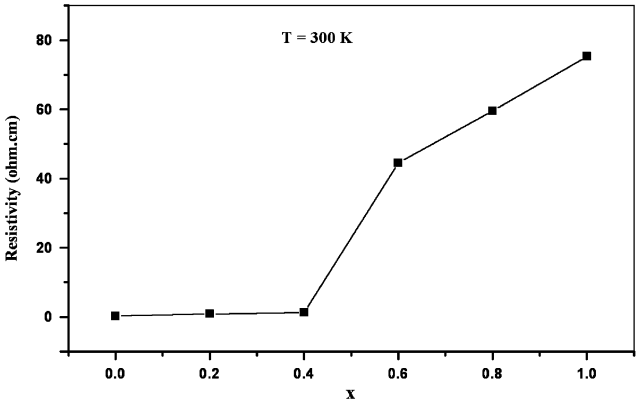

Fig. 7. Room temperature electrical resistivity as a function of Copper content in $NdSrNi_{1-x}Cu_xO_{4-\delta}$. Continuous line is a guide for the eye.

compound. In the present work, when substituting Ni^{3+} by Cu^{2+}/Cu^{3+} (electronic configuration $t_{2g}^6 d_{z^2}^2 d_{x^2-y^2}^1$/ $t_{2g}^6 d_{z^2}^2 d_{x^2-y^2}^0$) the half-filled $\sigma^*_{x^2-y^2}$ band changed progressively to a filled $\sigma^*_{z^2}$ band due to the presence of Cu^{3+} cation and consequently the resistivity increases with the incorporation of the Cu^{2+}/Cu^{3+} cation.

4. Conclusion

In summary, we have synthesized by solid-state reaction a new solid solution of $NdSrNi_{1-x}Cu_xO_{4-\delta}$, $0 \leqslant x \leqslant 1$, compositions, and studied their structural and electrical properties. Refinements of powder X-ray diffraction data show that these phases crystallize in the tetragonal K_2NiF_4-type structure ($I4/mmm$ space group) as predicted from tolerance factor consideration. Oxygen content deduced from TGA under reducing atmosphere indicated substantial deviations from the ideal values with the incorporation of Cu^{2+}/Cu^{3+} cation in the structure. A neutron powder diffraction study is now in progress to determine accurately oxygen positions and stoichiometry. The a and c unit cell parameters values displayed variations with increasing copper content, suggested from the Jahn–Teller distortions and presence of the mixed valence of the Cu^{2+}/Cu^{3+} ions.

An analysis of the micro-structure of $NdSrNi_{1-x}Cu_xO_{4-\delta}$, $0 \leqslant x \leqslant 1$, has been studied, and the crystallites sizes were deduced from X-ray diffraction profile refinement. The results mentioned that the crystallite size increases with copper content. The micro-structural results obtained from profile analysis of diffraction patterns are in agreement with those observed by scanning electron microscopy.

Electrical resistivity measurements indicated a gradual change in the transport properties from metallic in $NdSrNiO_{4-\delta}$ to semi-conducting behavior with progressive increase of Cu^{2+}/Cu^{3+} content.

Acknowledgments

The authors are indebted to J. Rocherulle (UMR.6512, Rennes) for technical assistance and fruitful discussions in TGA. T. Bataille and T. Guizouarn (UMR 6511, Rennes) are acknowledged for their contributions to X-ray diffraction data collection and electrical measurements, respectively.

References

[1] J.M. Bassat, P. Odier, F. Gervais, Phys. Rev. B 35 (1987) 7126.
[2] D.J. Buttrey, J.M. Honig, J. Solid State Chem. 72 (1988) 38.
[3] W. Bernard, D. Marc, C. R. Acad. Sci. C 267 (1968) 1482.
[4] U. Lehmann, Hk. Muller-Buschbaum, Z. Naturforsch. B 35 (1980) 389.
[5] G. Payom, M. Daire, Rev. Chim. Miner. 14 (1977) 11.
[6] G. Demazeau, M. Pouchard, P. Hagen Muller, J. Solid State Chem. 18 (1976) 159.
[7] B.W. Arbuckle, K.V. Ramanujachary, Z. Zhang, M. Greenblatt, J. Solid State Chem. 88 (1990) 278–290.
[8] J.G. Bednorz, K.A. Müller, Z. Phys. B 64 (1986) 189–193.
[9] E.E. Alp, G.K. Shenoy, D.G. Hinks, D.W. Capone II, L. Soderholm, H.-B. Schuttler, J. Guo, D.E. Ellis, P.A. Montano, M. Ramanathan, Phys. Rev. B 35 (1987) 7199–7202.
[10] Z. Kakol, J. Spalek, J.M. Honig, J. Solid State Chem. 79 (1989) 288.
[11] J. Gopalakrishnan, G. Colsmann, B. Reuter, J. Solid State Chem. 22 (1977) 145.
[12] Y. Takeda, R. Kanno, M. Sakano, O. Yamamoto, M. Takano, Y. Bando, H. Akinaga, K. Takita, J.B. Goodenough, Mater. Res. Bull. 25 (1990) 293.
[13] A.B. Austin, L.G. Garreiro, J.V. Marzik, Mater. Res. Bull. 24 (1989) 639.
[14] Y. Takeda, M. Nishijima, N. Imanishi, R. Kanno, O. Yamamoto, M. Takano, J. Solid State Chem. 96 (1992) 72.
[15] B.W. Arbuckle, Z. Zhang, M. Greenblatt, Chem. Electron. Ceram. Mater. (1990) 207.
[16] J. Rodriguez-Carvajal, Abstracts of the meeting Powder Diffraction, Toulouse, France, 1990, p. 127.
[17] J. Rodriguez-Carvajal, IUCr-CPD NewsLett. 26 (2001) 12.
[18] J. Rodriguez-Carvajal, T. Roisnel, Mater. Sci. Forum 443–444 (2004) 123–126.
[19] T. Roisnel, J. Rodriguez-Carvajal, Mater. Sci. Forum 378–381 (2001) 118–123.
[20] L.J. Van der Pauw, Philips Res. Rep. 13 (1958) 1.
[21] J.T. Lewandowski, R.A. Beyerlein, J.M. Longo, R.A. Mccauley, J. Am. Ceram. Soc. 69 (1986) 699.
[22] P.H. Labbe, M.L. Gilbert, V. Caignaert, B. Raveau, J. Solid State Chem. 91 (1991) 362–369.
[23] S.C. Chen, K.V. Ramanujachary, M.M. Greenblatt, J. Solid State Chem. 105 (1993) 444.
[24] V.M. Goldschmidt, Acad. Oslo I. Mater. Natur. 2 (1926) 7.
[25] P. Ganguly, C.N. Rao, J. Solid State Chem. 53 (1984) 193.
[26] R.D. Shannon, Acta Crystallogr. Sect. A 32 (1976) 751–767.